

## **Report**

This PD2 project is related to OTKA PD1 no.104334. The aim of the present proposal was to finance my postdoctoral employment and therefore its subject and this report overlap with OTKA 104334. For this reason only the OTKA104334 project is indicated in the papers.

## **Background**

One of the key components of the sustainable agriculture is the supplement of the soil with required amount of combined nitrogen in an environmentally friendly way. In the nature, the significant amount of the fixed nitrogen is provided by symbiotic and non-symbiotic biological nitrogen fixation. The most effective way of the biological nitrogen fixation is the endosymbiotic interaction between legume plants and soil bacteria, termed rhizobia. In this interaction, the plants provide carbon sources for the bacteria and rhizobia supply the host plant with fixed nitrogen in exchange. The symbiotic interaction results in the formation of a completely novel plant organ, the root nodule, wherein the reduction of the atmospheric nitrogen gas takes place. The formation and functioning of nitrogen fixing symbiosis requires a series of highly regulated and coordinated events and controlled by diverse factors and gene products. Mutants of both partners provide excellent tools to dissect the symbiotic interaction.

The main scientific interest of the Plant genomics and plant-microbe interaction group in NARIC is the study of the later stages of the nitrogen fixing symbiotic association between *Medicago truncatula* and *Sinorhizobium meliloti*. In our previous project supported by OTKA (NF67576), eight nodule function deficient (Fix-) mutant lines were analyzed and selected for gene cloning experiments (Domonkos et al 2013). One of these mutants, *epr* (enhanced pathogen response) was selected for this PD OTKA project. Preliminary experiments showed that in the *epr* mutant the nodule formation was arrested and signs of activated plant defense appeared. During the project we demonstrated the induction of defense responses, isolated and proved the mutated *EPR* gene. We attempted to identify which signaling pathway of the plant defense is activated in the *EPR* deficient plants, namely in which step *EPR* can block the defense response in cortical plant cells during the formation of symbiotic nodules.

## **Phenotypic characterization of the *epr* mutant**

Microscopic analysis was carried out to define at what stage of the nodule development is blocked in the *epr* mutant. Images showed that the nodule development

induced in similar way as in wild-type (wt) roots: infection threads were also formed in *epr* nodules at 4 days post inoculation (dpi). But relative early in nodule development, at 8 dpi the *epr* mutant nodules contained abnormally thick cell walls with pigmentation, which is the main characteristic of this mutant. The wt and mutant nodules were colonized in a similar way at 6 dpi but later (from 8 dpi) the colonized cells disappear in the mutant nodules. At later time points (12, 14 dpi) the mutant phenotype was more visible. These results suggest that the product of the *EPR* gene may play following the nodule cells are invaded by the bacterial partner (Figure 1.)

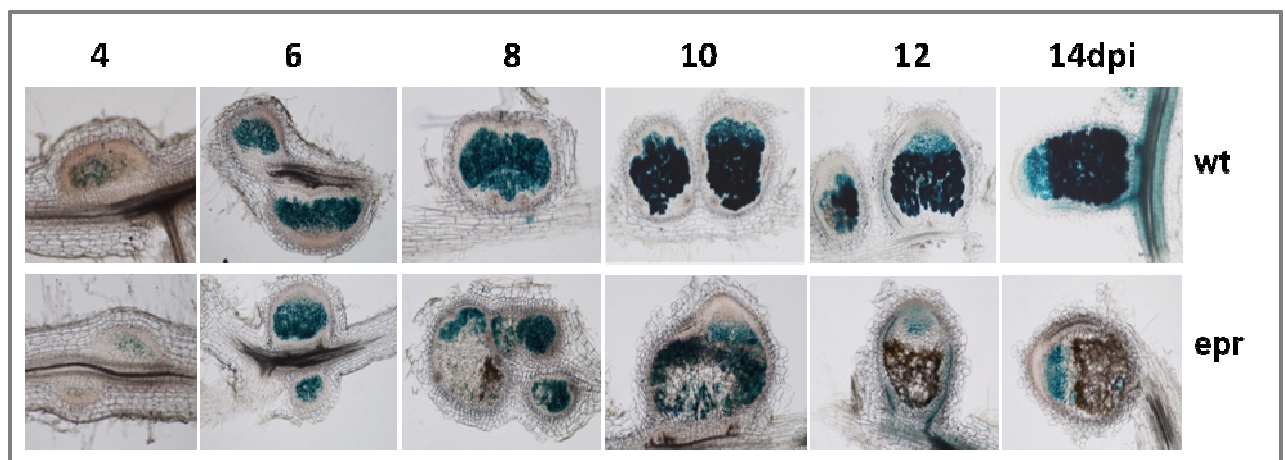


**Figure 1.** Semi-thin sections of *M. truncatula* wild-type and *epr* mutant nodules at different time points following inoculation with *Sinorhizobium medicae* strain WSM419 carrying the *LacZ* gene. The brown pigmentation appears 8 dpi and the rhizobia are eliminated during the progression of nodule development in *epr* nodules

### Identification of the position of *EPR* in the hierarchy of the genes involved in the symbiotic process

In order to examine the epistatic interaction of *EPR* and other *FIX* genes, double mutants were generated and analyzed for their symbiotic phenotype following rhizobium inoculation. Symbiotic mutants which are blocked at the stage of infection (*lin*), differentiation of rhizobia (*dnf1* and *dnf5*), or in nutrient exchange (symbiotic sulfate transporter1, *sst1*) and another symbiotic mutants, *dnf2* was crossed to *epr* and double mutants were generated.

In case of the *dnf 5-2/epr* double mutants, the nodulation phenotype shows both the earlier features of *dnf5-2* and *epr* nodules at 7 dpi (lack of enlargement of symbiotic cells and presence brownish pigments) but at later time point (14 dpi) the nodules of *dnf 5-2/epr* mutants resemble more to *epr*. These data suggest that DNF5 and EPR probably act in parallel pathways but later the activated defense response dominates the phenotype.

The phenotype of the single *dnf1* mutant nodules (Wang 2010) at 7 dpi resembles to wild-type nodules while *epr/dnf1* double mutant shows the phenotype of *epr* at 7 and 14 dpi. We concluded that function of the EPR protein precedes the functions of DNF-1 and the *EPR* gene acts prior the start of bacteroid differentiation.

The *lin/epr* double mutant shows the phenotype of *lin* (Kuppusamy 2004) indicating that *LIN* functions earlier than the product of *EPR*.

The nodules of *dnf2* and *epr* single mutants had very similar symbiotic phenotype, both mutants nodules accumulated pigments following rhizobial inoculation (Bourcy 2013). The *epr/dnf2* double mutants show similar cell wall thickening as the two single mutants that might indicate these two genes play role in the process of protection of rhizobia against the host pathogenic responses. (Figure 2.).

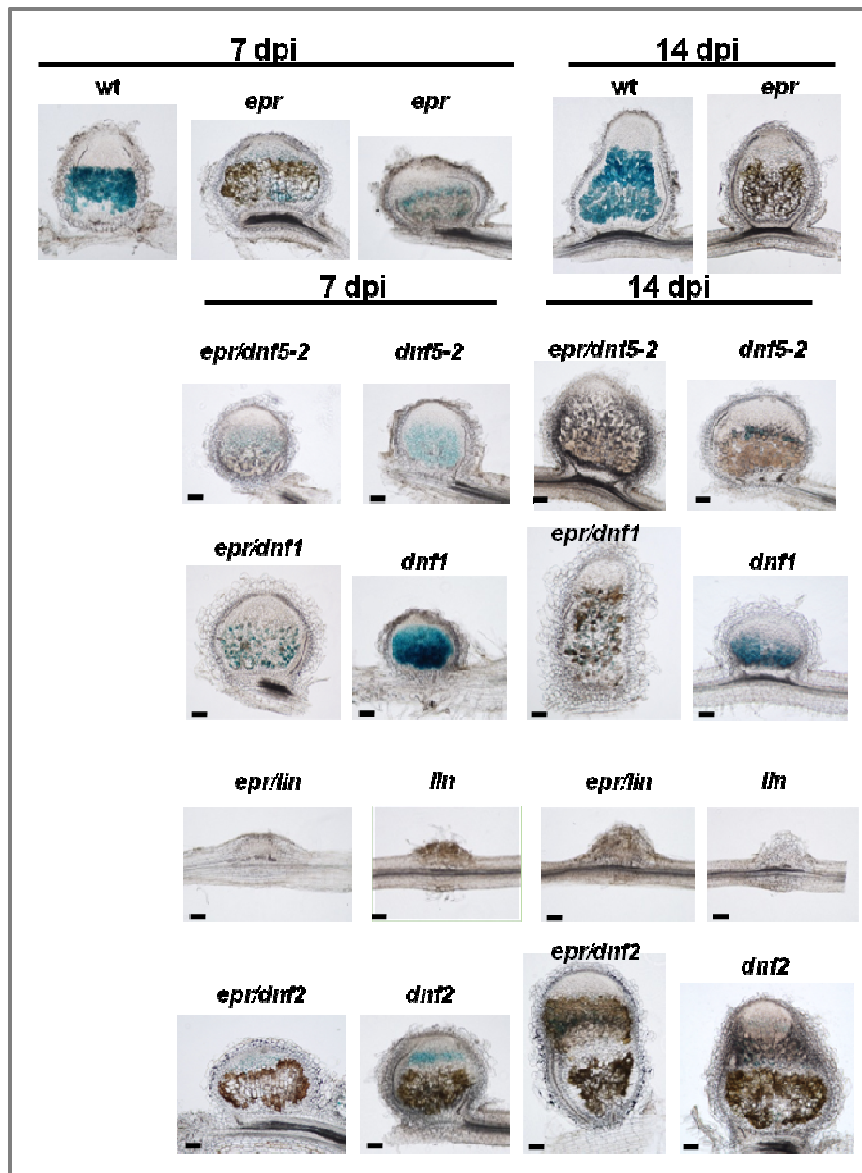


**Figure 2.** Sections of *M. truncatula* wild-type, *epr* and double mutants 7 and 14 dpi with *S. medicae* strain WSM419 constitutive expressing the *lacZ* gene

The *epr* mutant was inoculated with *S. meliloti* mutants deficient in exopolysaccharid production (*exoY* and *exoA*) or bacteroid differentiation (*bacA*) and wild type *S. meliloti* to define at what stage of symbiotic process is blocked.

The symbiotic interaction was arrested in wt plants corresponding to the mutant rhizobia strain used for inoculation. In the *epr* mutant plant, the rhizobia lacking the *exoA* and *exoY* genes displayed the same mutant phenotype as it was detected in wide type plants. The deficiency of *bacA* has no effect on the phenotype of *epr* mutant nodules; the similar accumulation of polyphenolics in the nodules is visible. This phenotype indicates that the *epr* mutation probably blocks the symbiotic process earlier than the rhizobial *bacA* functions, but following the function of bacterial *exoY* and *exoA* proteins. (Figure 3.)

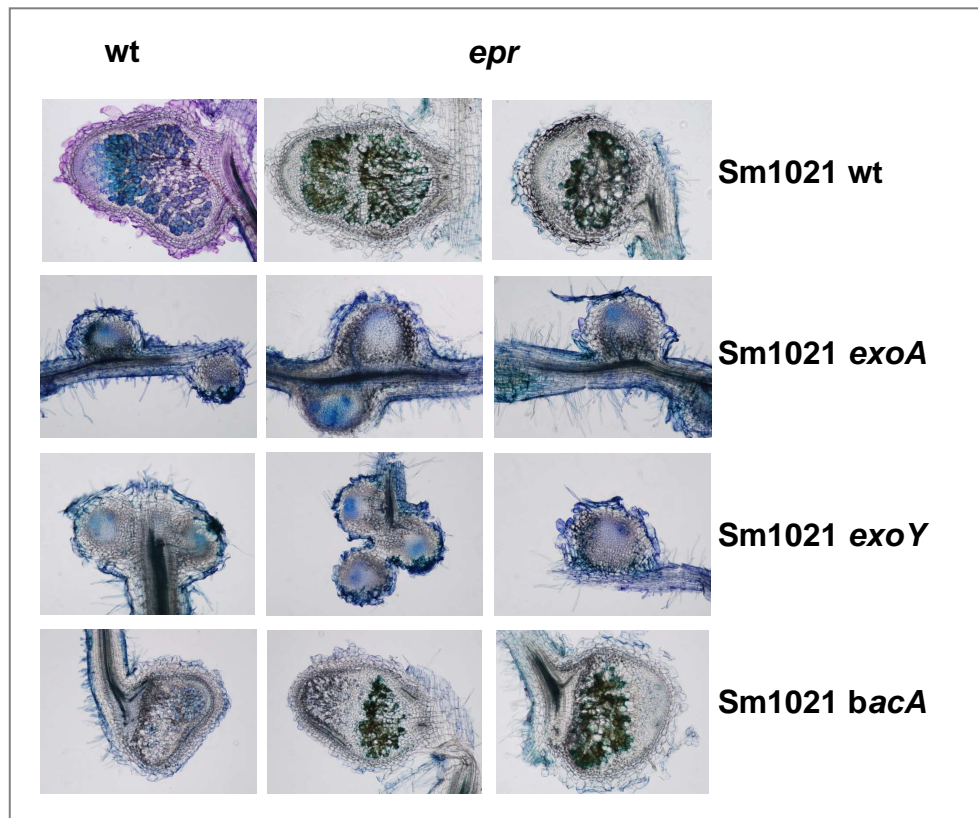


**Figure 3.** Sections of *M. truncatula* wild-type and *epr* mutant nodules 21 dpi with *S. meliloti* 1021 wt and its deletion derivatives. Nodules were stained with toluidine blue.

The nodulation process is blocked in wt plants inoculated with the mutant rhizobia as it was found in earlier studies. In the *epr* mutant, the rhizobia lacking the *exoA* and *exoY* genes displayed the mutant phenotype like in wt plants. The deletion of *BacA* has no effect on the phenotype of *epr* mutant nodules; the similar greenish blue staining appeared indicating the accumulation of polyphenolics in the nodules. This phenotype suggests that the symbiotic process is blocked earlier in *epr* than the rhizobial *BacA* functions.

Following the identification of the *EPR* gene (see below), we tested its expression in wt plants following wt and mutant rhizobia inoculation. In agreement with the microscopic

studies we observed that the EPR expressed only in the nodules induced by the *bacA* mutant and wt rhizobia but it was not induced in nodules or roots elicited earlier rhizobial mutants (*nodA* and *exoY*) nodules. This data further confirmed that EPR plays earlier than the rhizobial *BacA* functions. (Figure 4.)

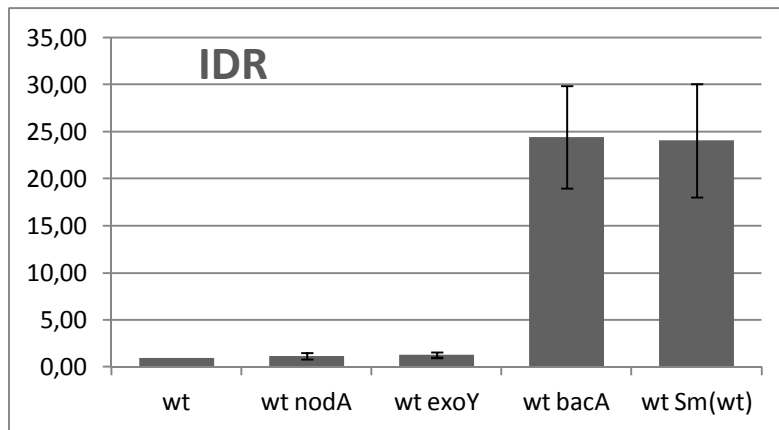


**Figure 4.** Relative expression of the *EPR* gene in *M. truncatula* wild-type plants 14 dpi with *S. meliloti* 1021 wt and its mutant derivatives. RNA were collected from root (ctrl, *nodA*) or nodules (*exoY*, *bacA* and wt).

### Autofluorescence

Jemalong (wt) and *epr*, *epr/dnf2* and *dnf2* mutant plants were analyzed by microscopy 14 days following rhizobia inoculation. The two single mutants and the double mutant displayed the typical accumulation of pigments in the nodules. Using confocal laser scanning microscopy, extreme high autofluorescence appeared in the mutant nodules irrespectively of the mutant we tested. These results confirm the fact that these mutants respond to rhizobia with induced defense reaction.

We stained the nodule sections with SYTO 13 fluorescence DNA stain to follow the bacteroid differentiation process. The results show that no living bacteria could be detected in the nitrogen fixing zone though the bacteroid differentiation is initiated at reduced level in the interzone, where the bacteria enter the plant cells and terminal differentiation occurs in the wt plants. (Figure 5.)

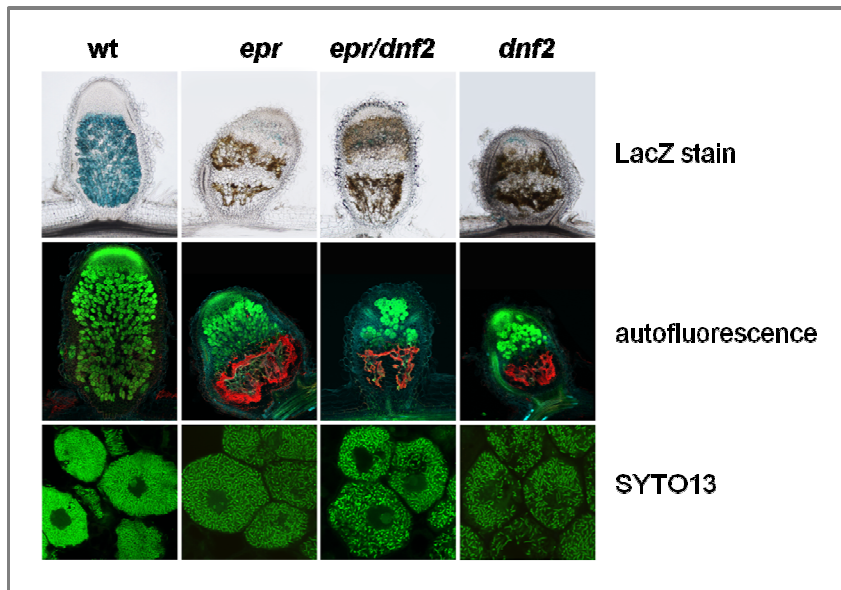


**Figure 5.** LacZ and SYTO13 staining of wt, *epr*, *epr/dnf2* and *dnf2* mutants indicate the colonization of mutant nodules and the initiation of rhizobial differentiation. Mutant nodules display strong autofluorescence in the zone corresponding to the nitrogen fixation zone of wt nodules.

### Analysis of the ultrastructure of the mutant nodules

Electron microscopic studies showed that the autofluorescent cells are devoid of cytosol, membranes and cell particles were collapsed and cell wall were thickened. As a result of massive defense response most cells are died in the nitrogen fixation zone, living cells can be hardly found in this region. This data also indicate that the control over the defense responses against rhizobia were lost due to the missing *EPR* gene product (Figure 6.).

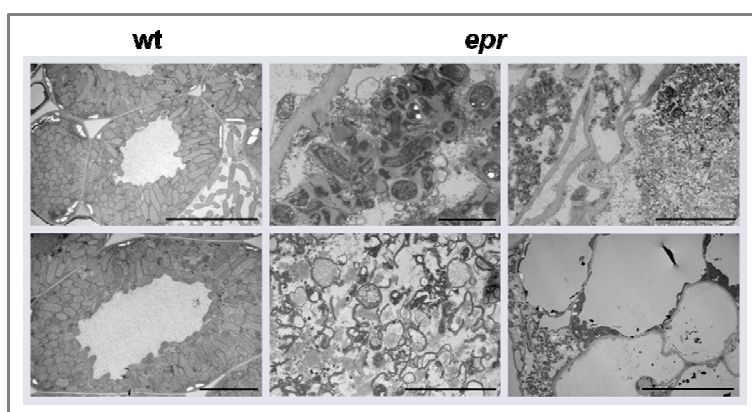


**Figure 6.** Electron microscopic images of nodule cell of wt and *epr* mutant (bars are 10 and 2  $\mu$ m)

## Isolation of the *EPR* gene

The *EPR* gene was identified by map-based cloning. The mutant locus was positioned on the upper arm of chromosome 7 (LG 7) between markers Mtb249 and Mtb186 by genetic mapping. Further fine mapping positioned the locus in a genomic region with a size of 153 kbp containing 24 genes. Searching for deletion in the region identified a gene (Medtr7g022640) with unknown function that was affected in the *epr* (7Y) mutant. The sequence analysis of the mutant showed a fifty basepair-long deletion in the first intron of the gene (annotation in *Medicago truncatula* Genome Project v4.0). Prediction was based on a single EST (Genebank ID BG582085) encoding a peptide of 68 amino acids.

In order to prove the gene identity, genetic complementation was carried out. The Medtr7g022640 gene was introduced into mutant plants by *Agrobacterium rhizogenes* mediated transformation. Composite plants were checked for nodulation following rhizobium inoculation. The development of wt nodules and nitrogen fixing ability of the nodules on transformed *epr* roots proved the identity of the *EPR* gene. (Figure 7.)

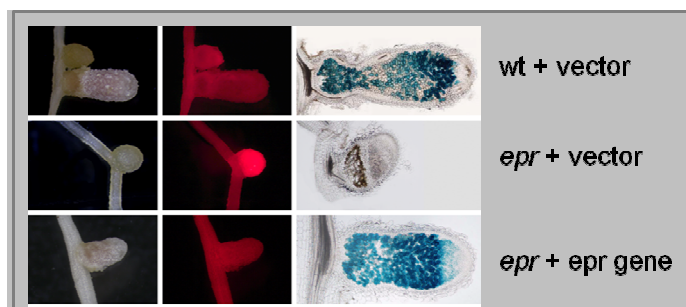


**Figure 7.** Complementation experiments with the whole *EPR* gene

In order to prove that the deletion in the predicted first intron caused the deficiency of Medtr7g022640, we carried out further complementation experiments using the *A. rhizogenes* hairy root transformation system with four different constructs containing the genomic region of the gene with or without the first intron. The complementation experiment showed that only the complete genomic region could revert the wide type phenotype for *epr* mutant perfectly. (Figure 8.)

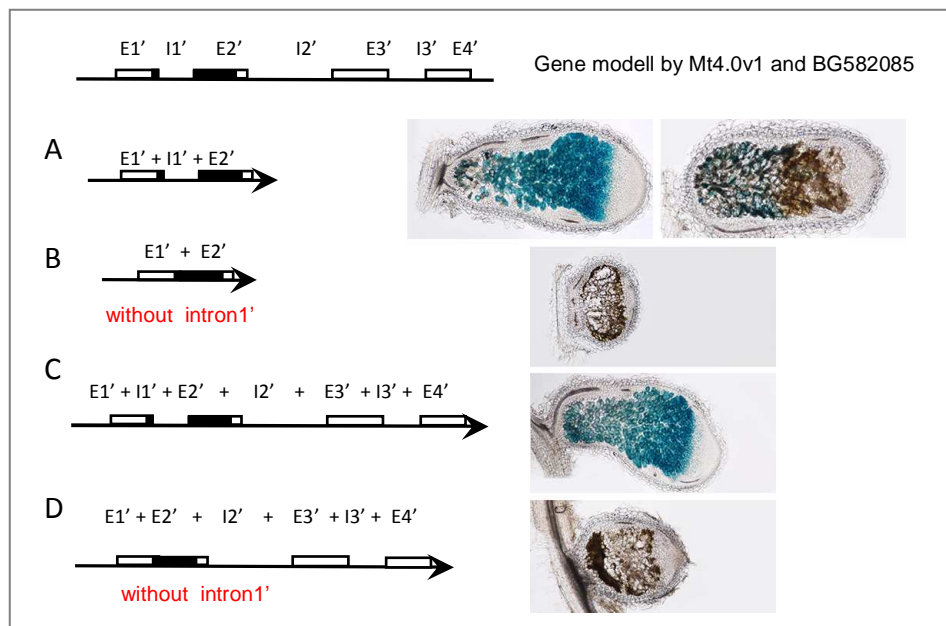


**Figure 8.** Complementation experiments to prove the exons and introns in the *Medtr7g022640* gene

**A.** the predicted (Mt4.0v1) first two exons (1' and 2') with intron 1'

**B.** the predicted first two exons without intron 1'

**C.** the predicted four exons with all the introns

**D.** the predicted four exons without intron 1' but with intron 2' and 3'

Only the complete genomic region could revert the wide type phenotype of the *epr* mutant perfectly. We found wild type nodules occasionally on transformed roots of *epr* plants using construct (panel A) too but the complementation was less efficient comparing to the construct of panel C. (Scale bars = 200  $\mu$ m)

According to the annotation found in the *Medicago* genome database (<http://medicago.jcvi.org/medicago/index.php>), the *Medtr7g022640* (*MTR\_7g022640*) gene (*EPR*) consists of 4 exons and 3 introns encoding a 71 amino acid long putative protein containing with transmembrane domains (*Medicago Truncatula* Genome Project) or as a hypothetical protein (NCBI). The mutant gene in *epr* contained a 50 nucleotide long deletion in a predicted intronic region. Our expression studies followed by sequence analysis of the *Medtr7g022640* in *epr* mutant and wild type plants detected none of the predicted short introns (I1' and I3') suggesting that *Medtr7g022640* consists of only two exons and a long single intron. Both exon 1 and 2 were present on all the tested *Medtr7g022640* transcripts. Based on these results we concluded that the originally predicted (Mt4.0v1) intron 1' is not excised under the condition we used and we presume that former exon 1', intron1' and exon 2' compose a single exon. Analyzing the sequence of exon 1 and 2 predicts an ORF in exon1 that encodes a 96 amino acids long peptide. (Figure 9.)

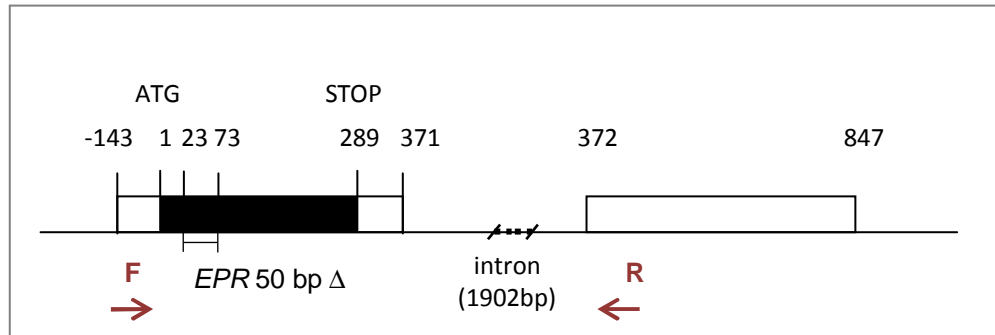
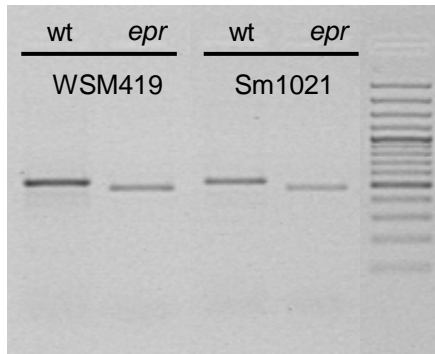


**Figure 9.** Two predicted intronic regions (one containing the deletion) were present on the cDNA prepared from the wide type plants. New gene model predicts a single intron for the Medtr7g022640 gene.

We concluded that the Medtr7g022640 gene contains only 2 exons (instead of the predicted 4) encoding a protein of 96 amino acid residues with two transmembrane domains. We could not find any alternative splicing site but we detected alternative polyadenylation sites.

### Gene expression studies

After isolation the *EPR* gene (Medtr7g022640) and a successful complementation experiment, we analyzed the expression of *EPR* in rhizobium inoculated *M. truncatula* roots. RNA was isolated at different time points after inoculation the plants with *S. medicae*. The expression of the *EPR* gene was monitored by quantitative RT-PCR. We proved the nodule-specific expression of *EPR* and the time scale experiments showed that the gene is induced already at 4 dpi. The highest expression level of *EPR* was detected between days 7 and 21 and the expression slightly decreased following 28 dpi (Figure 10.).

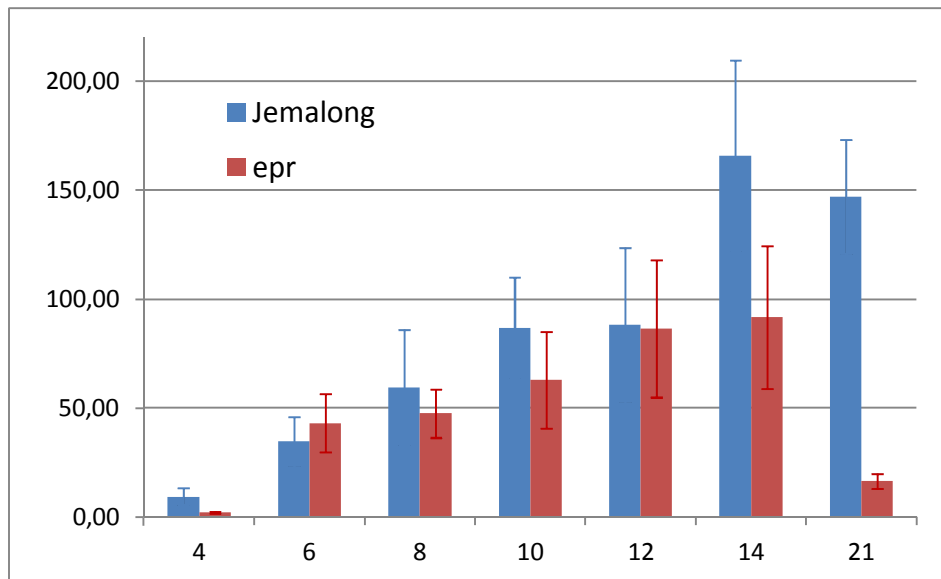


**Figure 10.** Temporal expression of Medtr7g022640 (*EPR*) in wt and *epr* mutant following inoculation with rhizobia

### Whole transcriptome shotgun sequencing (WTSS)

Two runs of WTSS of the *epr* mutant were carried out on SOLID platform. RNA samples were prepared from nodules of *epr* and wild-type plants 14 dpi with rhizobia. The expression of 1232 genes changed significantly out of the tested 44148 gene models. We found the up-regulation of several defence-related genes in the *epr* mutant with RNAseq and confirmed the upregulation of eleven defence response genes by qRT-PCR in *epr*, *dnf2* and also in *epr/dnf2* double mutant.

Upregulation of some other genes were tested also by qRT-PCR. The gene products of the flavonol synthase and plant invertase genes are involved in the accumulation of polyphenols characteristic of *epr* mutant. Activation of both genes was validated. Extreme upregulation of Kunitz-type tripsin inhibitors was also confirmed in the *epr* mutant (7Y), *dnf2* and the double mutant. This tripsin inhibitor (Medtr6g078250) is highly activated under pathogen attack in legumes.

In contrast the upregulation of ACC oxidase, the enzyme involve in ethylene biosynthesis was not proven. This fact suggests, that ethylene signaling is probably not the main participant in the activation of defence response in the *epr* mutant. (Figure 11.)

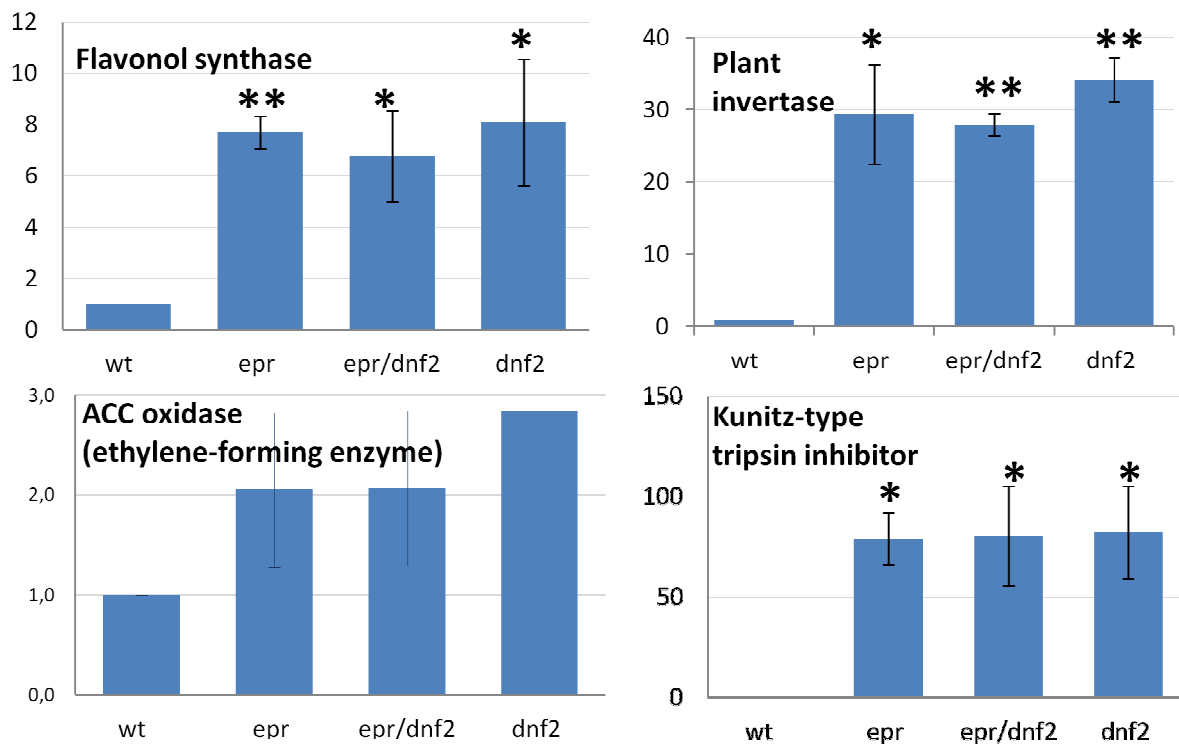


**Figure 11.** Confirmation of expression of genes selected from WTTS data (\*\*- P<0,01; \*- P<0,05)

### Comparison of defence response and developmental senescence

The deficiency of ineffective symbiosis generally triggers the early senescence of the symbiotic nodule. In order to differentiate between defence responses induced by pathogenic or saprophytic microbes and developmental senescence, we compared the symbiotic phenotype of *epr* (7Y), *11S*, *5L* (both symbiotic sulfate transporter1 mutants, *sst1-2* and *sst1-1*), *6V* (*dnf7-2*), *13U* (putative Fe transporter mutant) and *dnf4* mutants. *6L* is a root developmental mutant, which nodulates similarly as wt plants. We have followed the transcriptional activation of some genes referred as either senescence or/and defence related genes at 14 dpi in all of the  $\text{Fix}^-$  mutants wherein symbiosis is blocked due to the incomplete differentiation of bacteroids (*6V* and *dnf4*) or insufficient transport function. The expression of five marker genes was analyzed by qRT-PCR. A cysteine proteinase (Medtr5g022560) and chitinase2 (Medtr6g079630) genes associated with senescence were highly up-regulated in all of the mutants. Genes associated with defence responses, such as the *NDRI* (a Non-race-specific Disease Resistance Medtr5g076170), *PR-10* (Medtr2g035150) and hevein, another chitinase gene (Medtr3g118390) were not induced in all the symbiotic mutants but they were highly expressed in *epr*. These data are in agreement with the massive defence-like reaction

detected in *epi* mutant that precedes the developmental senescence which is characteristic for the other fix- mutants (Figure 12.).

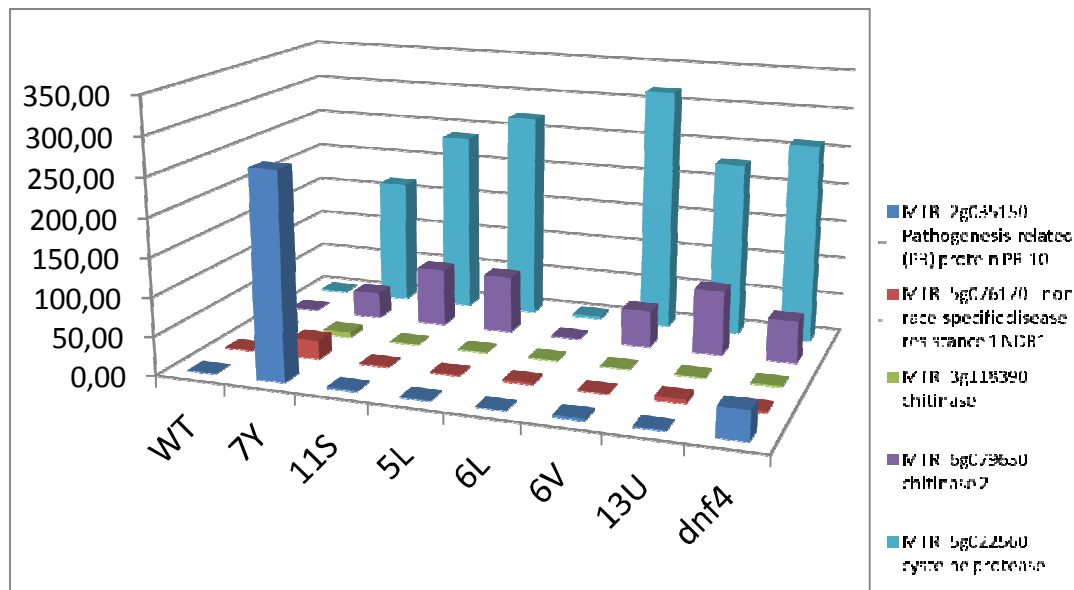


**Figure 12.** The expression of marker genes of defence and senescence processes was monitored at 14 dpi in 7Y (*epi*) and other ineffective symbiotic mutants identified earlier (Starker et al. 2006, Plant Phys. 140:671; Domonkos et al. 2013, BMC Plant Biol. 13:157) and wt symbiotic plants (wt and 6L). The analysis revealed that the chitinase 2 (MTR\_6g079630) and cysteine protease (MTR\_5g022560) genes had extremely high expression in all the nodulation mutants compared to wt except a root morphogenic mutant (6L) with functional symbiotic nodules which expression pattern for these genes was similar to wt. The 7Y mutant was unique among them in showing extreme high transcript level of the pathogenesis-related protein 10 and also substantially higher expression level of a non-race-specific disease resistance 1 (*NDR1*) gene compared to wt.

We followed the temporal induction of these senescence or/and defence-related genes in the *epi* mutant 4, 6, 8, 10, 12 and 14 dpi compared to the wt. All the tested genes showed enhanced relative expression level from 6 or 8 dpi compared to wt corresponding to the appearance of the hallmarks of the pathogen responses detected in the mutant nodules (Figure 13.). The expression level of the genes was monitored at the same time points following inoculation with rhizobia as for the analysis of the LacZ stained semi-thin sections on Figure 1.

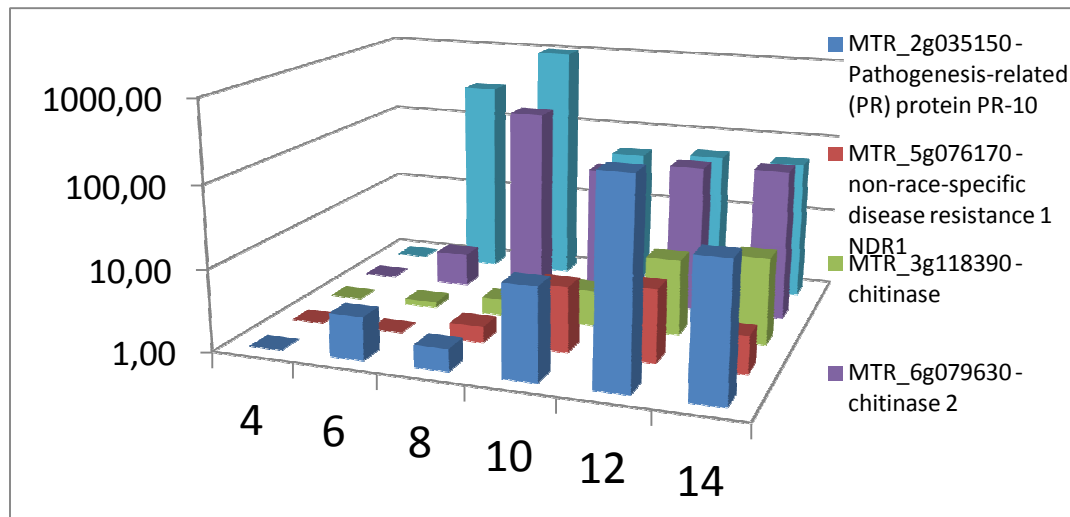


**Figure 13.** The expression level of genes associated with pathogens responses or senescence of the nodules at different time points in *epr* compared to wt.

### Characterization of *EPR* gene and functional analysis of the gene product

We created a construct of the native promoter of *EPR* gene fused with GUS reporter to monitor the tissue specificity of the *EPR* gene expression. Using the *A. rhizogenes*-mediated transformation system, we created chimera Jemalong plants with transgenic roots. The analysis of the nodule sections of transformed roots was stained for  $\beta$ -glucuronidase activity. We found that the *EPR* promoter was active in the proximal part of the invasion zone, interzone and nitrogen fixation zone of the nodules. These results corresponded to the expression pattern of *EPR* obtained from RNA seq data (Roux et al 2014).

Other constructs consisting of the native promoter and coding sequence of *EPR* fused to the GFP reporter gene, same construct with C terminal c-myc tag, or N terminal GFP-EPR under the control of EF1 promoter of *Arabidopsis thaliana* were introduced into the *epr* mutant plants via the *A. rhizogenes* transformation system. Unfortunately none of the GFP-fusion constructs nor the myc-tagged construct were able to rescue the mutant phenotype. We do not know yet why these fusion constructs interfered with the complementation capacity of the constructs. In the case of GFP we can explain with the size of the reporter, which is more than two times bigger, than the EPR protein. In the case of c-myc-tag the size of the fusion protein is less likely but it is possible that all tags interfere with the secondary structure of functional EPR.

In order to test whether EPR functions in the control of defence response upon pathogen attack, we attempted to analyse the phenotype of *epr* following inoculation with the root pathogen *Ralstonia solanacearum*. We tried different inoculation systems for cultivating and infecting the plants but the experimental data we observed were not reproducible.

Part of the results describing the difference in developmental senescence and defence-related processes was published in a PNAS paper. The preparation of manuscript describing the *epr* mutant, the cloning of the *EPR* gene and its detailed characterization is in progress.

Beatrix Horváth, **Ágota Domonkos**, Attila Kereszt, Attila Szucs, Edit Ábrahám, Ferhan Ayaydin, Károly Bóka, Yuhui Chen, Rujin Chen, Jeremy D. Murray, Michael K. Udvardi, Éva Kondorosi, and Péter Kaló 2015. Loss of the nodule-specific cysteine rich peptide, NCR169, abolishes symbiotic nitrogen fixation in the *Medicago truncatula dnf7* mutant. PNAS 112:(49) pp. 15232-15237.)

Domonkos Ágota